Antiferromagnetic spin-coupling between Mn^{II} and amminium radical cation ligands: models for coordination polymer magnets

Richard J. Bushby*, Colin Kilner, Norman Taylor and Rhidian A. Williams

Self-Organising Molecular Systems (SOMS) Centre and School of Chemistry, University of Leeds, Leeds, LS2 9JT.

---

* Corresponding author.
E-mail address: r.j.bushby@leeds.ac.uk

Abstract

One and two electron oxidation of the manganese(II) complex $[L_2Mn(hfac)_2]$ {L = 4",4'"-di-*tert*-butyl-2',2",2'"trimethoxy-{4-(4'-diphenylaminophenyl)pyridine} were studied by ultra violet/ visible/ near infra red spectroscopy, cyclic voltammetry and magnetometry. A one-electron oxidation converts the triarylamine ligand to its radical cation and gives a complex in which the antiferromagnetic coupling between the spin on the ligand and that on the metal J/k_b is -1.5 K. In a dilute frozen matrix and at low temperature this behaves as an S = 2 system. A two electron oxidation gives $[L_2Mn(hfac)_2]^{2.+}$ which at low enough temperatures behaves as an S = 3/2 system but the spin-coupling between the metal and the ligand is weaker (J/k_b = -0.3 K). The weakness of these spin-couplings mean that Mn^{II}/amminium radical cation complexes are not promising systems on which to base coordination polymer magnets. The equivalent copper(II) complex $[L_2Cu(hfac)_2]$ was also investigated but this decomposes when an attempt is made to oxidise the ligand to its amminium radical cation.

Keywords: Manganese(II); Copper(II); Molecular magnet; Crystal structures

1. Introduction

One of the most successful strategies for producing molecular magnets is that originally pioneered by Gatteshi [1, 2] which relies on the creation of coordination polymers in which spin-bearing ligands and spin-bearing transition metal centres alternate with each other. At low enough temperatures, such systems can show bulk magnetic properties regardless of whether the coupling between metal and ligand is ferromagnetic or antiferromagnetic [2]. Systems of this type include a vanadium/TCNE complex which has a Curie temperature which is above room temperature but in most such systems there is weak or very weak spin-coupling between the ligand and the metal and, as a result, Curie temperatures are also low [3]. Most other examples exploit nitroxide [4] or nitronyl nitroxide [2, 5] as the spin-bearing ligand although several others have been investigated [6, 7]. This paper explores the possibility of using amminium radical cation ligands. We have used the monopyridyl functionalised triarylamine ligand **3** to make the model 'monomers' **4** and **5** (Scheme 1) and then tried to oxidise the ligands to the amminium radical cation level. The sign of the spin coupling between the ligand radical cation and the metal ion centre in the resulting $\mathbf{4}^{n,+}$ and $\mathbf{5}^{n,+}$ complexes is expected to depend on whether the spin orbitals overlap or are orthogonal [7]. In the Mn^{II} complexes the non-zero overlap between spin orbitals should result in an antiferromagnetic interaction but, in the case of the copper complex the spin orbitals are orthogonal and the interaction should be ferromagnetic [8].

2. Results

2.1. Synthesis and X-Ray crystal structures

As shown in Scheme 1, the ligand **3** was prepared by a Suzuki coupling reaction between the monoboronic acid **2** (from the bromocompound **1** [9]) and 4-bromopyridine. The required 2:1 complexes **4** and **5** were obtained by mixing solutions of the ligand with $[Mn(hfac)_2]$ or $[Cu(hfac)_2]$. Recrystalisation of the complexes **4** and **5** from THF/hexane gave orange and green crystals respectively. Single crystal X-ray structures were obtained for all three compounds **3-5**, the derived molecular structures are shown in Fig. 1 and crystal structure refinement data is given in the experimental section and Table 1. As expected, ligand **3** shows a propeller-like twist of the aryl residues around an almost planar central nitrogen. Like other triarylamines, the dihedral angles range between 53° and 74°. The torsional angle between the pyridine and benzene rings of 36° is also similar to that in related compounds [10]. As expected, the geometry of the ligand is only slightly changed on forming the complexes **4** and **5** and complexation occurs through the pyridyl rather than arylamine nitrogen. The Mn complex **4** has dihedral angles between 56° and 68° with a torsional angle of 29° and in the Cu complex **5** the dihedral angles range between 56° and 69° with a torsional angle of 31°.

2.2. Cyclic voltammetry

A cyclic voltammogram for the ligand **3** is shown in Fig. 2 [11]. There is a clean one-electron redox process at 0.71 V (versus silver/silver chloride) with a width at half height of about 0.1V. Both forward and reverse scans match in amplitude and there are no additional peaks of the type associated with benzidine formation, even after many cycles [10]. This indicates that a fast reversible electrochemical process is occurring and that the amminium radical cation $\mathbf{3}^{\cdot+}$ is chemically stable on the CV timescale. Both of the complexes **4** and **5** show oxidation potentials and peak widths

that are essentially the same as those of the uncomplexed ligand **3** [12]. This is the first indication that oxidation is occurring at the ligand rather than at the metal centre: something that is confirmed by the spectroscopy and magnetometry studies described below. This is not surprising since oxidation of manganese(II) to manganese(III) in similar complexes is known to require much higher potentials [13]. If each of the ligands in turn is being oxidised to the radical cation level and the complex remains intact (for example, **4,** $[Ar_3N\ Mn^{II}\ Ar_3N] \rightarrow$ $\mathbf{4^{\cdot+}}$, $[Ar_3N^{\cdot+}\ Mn^{II}\ Ar_3N] \rightarrow \mathbf{4^{2.+}}$, $[Ar_3N^{\cdot+}\ Mn^{II}\ Ar_3N^{\cdot+}]$) one could argue that there should be shifts in ligand oxidation potentials arising from coulombic repulsion between the charge on the ligand and that on the metal ion (as in $\mathbf{4^{\cdot+}}$) and between the charges on the two ligands (as in $\mathbf{4^{2.+}}$). However, the charged centres are well separated from each other and in dichloromethane these systems are strongly ion-paired so that the charge-charge repulsion is screened out by the counter-ion. Based on data reported by D. McGill [14] for related ion-paired dication diradical species in dichloromethane and given the separation between the charged centres (which is known from crystal structure data) the shifts in the oxidation potentials due to such coulombic repulsions would be < 25 mV. Such small differences would be difficult to observe and so the similarity of the CV data for complexed and uncomplexed ligands does not indicate whether or not the complexes remain intact.

2.3. Ultra Violet/ visible/ near infra red spectroscopic studies

These studies were carried out using thianthrenium tetrafluoroborate ($THBF_4$) as the oxidant [15]. This has the advantage of being dichloromethane soluble so that it can be used in a quantitative titration. The results of these titrations are shown in Fig. 3 and the numerical data are summarised in the experimental section. The electronic absorption

spectrum (250-1250 nm) for the neutral amine **3** in dichloromethane shows one main absorption band at 354nm. When it is oxidised with one molar equivalent of $THBF_4$ the spectrum is replaced by that of the radical cation $\mathbf{3}^{\cdot+}$ showing bands at 467, 620 and 920 nm. Because of the lowered symmetry the D_0-D_1 transition is split [10, 16]. There are sharp isosbestic points at 297 and 377 nm, indicating a clean oxidation. Relative to the uncomplexed ligand $\mathbf{3}^{\cdot+}$, the spectrum of the complex $\mathbf{4}^{\cdot+}$ (Fig. 3, bottom) is slightly shifted with the main absorption band at 370nm. On adding another equivalent of $THBF_4$, both of the ligands are oxidised to the radical cation level. The resulting diradical dication $\mathbf{4}^{2,+}$ shows three bands at 469, 619 and 925 nm. These changes parallel those for the uncomplexed ligand **3** but all of the bands are all slightly shifted. This confirms that the complex does not dissociate upon oxidation. There is a clean isosbestic point for the first one electron oxidation step although this is less clear for the second (Fig. 3, insets). Whereas the results for the oxidation of the ligand **3** and of the manganese complex **4** are straightforward and easy to interpret the results obtained for the copper complex **5** are not. As expected the electronic absorption spectrum for the neutral complex **5** in dichloromethane shows one main absorption band at 369 nm but on oxidation, using either $THBF_4$ or $NOBF_4$ as the oxidant, a complex series of changes occurs which is quite different to those normally associated with amminium radical cation formation. It appears that even though the amminium ion/copper complexes are stable on the short time-scale of the cyclic voltammetry experiments they are not stable on the longer time-scale of these spectroscopic studies.

2.4. Magnetometry

Magnetometry studies were carried out using dilute frozen solutions which were prepared by the mixture of syringe and vacuum line techniques described previously [9]. This

method minimises exposure to air during sample preparation and transfer, and requires less material than using dry powered samples. It also has the advantage that intermolecular spin interactions, which can complicate the interpretation of the data, can be ignored. The disadvantage is that, at higher temperatures, the signal becomes weak relative to the diamagnetic correction and the errors can be larger. Magnetic measurements were made on the neutral complex **4**, the monoradical monocation $\mathbf{4}^{\cdot+}$ and diradical dication complex $\mathbf{4}^{2,+}$. For the neutral Mn complex **4,** since we have a dilute frozen matrix, the individual manganese(II) S = 5/2 centres are expected to behave independently. It was found that the Curie law was obeyed and χT was 4.35 emu.K.mol^{-1} which is about the value expected for a dilute paramagnet of S = 5/2. This is confirmed by plots of the normalized magnetisation vs. the ratio of magnetic field and temperature (M/M_{sat} vs. H/T) which is consistent with a Brillouin function of S = 5/2 at both 2 and 5 K [12]. Magnetic data for the mono and diradical complexes were obtained by selectively oxidising the sample with one or two equivalents of $THBF_4$ respectively. For the monoradical monocation $\mathbf{4}^{\cdot+}$ the Curie law is obeyed. Hence the plot ($1/\chi$ vs. T) at low field (0. 5 Tesla) is linear as shown in Fig. 4 (top) and intercepts around 0 K. The product of susceptibility and temperature vs. temperature (χT vs. T) gradually increases from 2 K and flattens out around 50 K giving a high temperature χT value of 4.71 emu.K.mol^{-1} (Fig. 4, middle). This is close to the value expected for a system with isolated S = 1/2 and S = 5/2 spins. However, at low enough temperatures the spins are antiferromagnetically coupled and the system behaves as if comprised of isolated S = (5/2 – 1/2) = 2 spin centres. This is confirmed by plots of the normalized magnetisation vs. the ratio of magnetic field and temperature (M/M_{sat} vs. H/T) which fit reasonably closely to a Brillouin function of S = 2 (Fig. 4, bottom). The strength of the spin coupling (J_{ab}) was determined by fitting the χT vs. T curve using the Bleaney-

Bowers equation [17] for a system with an antiferromagnetic interaction between S = 5/2 and S = 1/2 spins [18].

$$\chi T = Ng^2\mu_B{}^2T/k_BT.\ [28 + 10\exp(-6J/k_BT)]/[7 + 5\exp(-6J/K_BT)] + N_\alpha$$

The experimental data best fits a weak intramolecular antiferromagnetic coupling of J/k_B = - 1.5 K. For the dication $\mathbf{4}^{2.+}$, the Curie law is obeyed, the plot ($1/\chi$ vs. T) at low field (0. 5 Tesla) is linear as shown in Fig. 5 (top) and intercepts around 0 K. The product of susceptibility and temperature vs. temperature (χT vs. T) gradually increases from 2 K and flattens out around 30 K giving a high temperature χT value of 5.06 emu.K.mol^{-1} (Fig. 5, middle). This value is close to that expected for a system with isolated S = 5/2 and a pair of isolated S = 1/2 spins. If, at low enough temperatures the spins are antiferromagnetically coupled we should get magnetically isolated S = (5/2-1/2-1/2) = 3/2 spin centres. This is confirmed by plots of the normalized magnetisation vs. the ratio of magnetic field and temperature (M/M_{sat} vs. H/T)which fit reasonably closely to a Brillouin function of S = 3/2 at 2 and 5 K (Fig. 5, bottom). The strength of the intramolecular coupling (J_{ab}) was determined by fitting the χT vs. T curve using the Bleaney-Bowers equation for a symmetrical (S = 1/2) – (S = 5/2) – (S = 1/2) system with antiferromagnetic coupling between the S = 5/2 and S = 1/2 centres and zero coupling between the two S = 1/2 centres [19].

$$\chi = \{Ng^2\mu_B{}^2T/4k_BT\}.\ \{[84\exp(5J/k_BT) + 35\exp(-2J/k_BT) + 10\exp(-7J/k_BT) + 35] / [4\exp(5J/k_BT) + 3\exp(-2J/k_BT) + 2\exp(-7J/k_BT) + 3]\} + N_\alpha$$

The experimental data best fits weak intramolecular antiferromagnetic coupling with a value of J/k_B = - 0.3 K (Fig. 5, middle).

For a dilute frozen solution of the neutral Cu^{II} complex **5** the Curie law is obeyed and the plot intercepts around 0 K indicating that there is negligible intermolecular interactions. χT is 0.39 emu.K.mol^{-1}; a value which is consistent with χT = 0.37 emu.K.mol^{-1} calculated for a dilute paramagnet of S = 1/2, indicating that the unpaired d electron of copper(II) is magnetically isolated. Plots of the normalized magnetisation vs. the ratio of magnetic field and temperature (M/M_{sat} vs. H/T) which is consistent with a Brillouin function of S = 1/2 at 2 and 5 K [12].

3. Discussion

It is very difficult to design a high-spin polymer that is purely organic [20, 21] because both the range of ferromagnetic coupling units [22] and the number of stable free radicals is very limited. On the other hand, coordination polymers allow us to exploit the d orbitals of stable metal complexes and because we can use two metals with different moments or a metal and ligand with different moments it is not even necessary to engineer ferromagnetic coupling. This is a much easier strategy. One way to view the relationship between the purely organic high-spin polymers and the coordination polymers is illustrated in Fig. 6. As can be seen, in terms of the spin-coupling pathways, either a transition metal centre or an organic ferromagnetic coupling unit (metaphenylene, 3,4'-disubstituted biphenyl or 4,4"-disubstituted metaterphenyl, etc.) [22] can have the same function. It mediates an overall ferromagnetic coupling between radical, radical ion or carbene centres. Hence, the copper(I) in **6** [23] has the same function of feromagnetically coupling perchlorotrityl centres as the tertrachlorometaphenylene in **7** [25]**,** the manganese(II) in **8** [26] has the

same function of coupling carbene centres as the metaphenylene in **9** [24] and the manganese(II) in **10** [27] has the same function of coupling triarylamminium radical cation centres as the 4,4"-disubstituted metaterphenyl in **11** [9, 14, 28] However, in all systems, whether purely organic or organometallic, the strength of the interaction is critical [9, 10, 21] Unfortunately, couplings are often weak and so low Curie temperatures result. In our work aimed at purely organic systems we used amminium ion spin-bearing centres ferromagnetically coupled 1,3 through benzene, 3,4'-through biphenyl or (mostly) 4,4"-through metaterphenyl [9, 10, 14, 28] In the present work we have explored the coupling of similar amminium ion spin-bearing centres through Mn^{II}. These were generated by one and two electron oxidation of a neutral triarlyamine/Mn^{II} complex **4**. The complex remained stable when the ligands were oxidised to the amminium ion level but the antiferromagnetic spin-coupling between amminium ion and Mn^{II} centres proved to be weak in the monoradical monocation $\mathbf{4}^{\cdot+}$ and weaker still in the diradical dication $\mathbf{4}^{2\cdot+}$. This seems to indicate a decrease in the overlap of the spin orbitals when the second electron is removed. A possible explanation is in terms of a space charge effect: that increased coulombic repulsion in the diradical dication leads to a small extension of the Mn–pyridyl bonds and a decrease in the d-π overlap. If space charge is indeed the cause it is clear that using radical ion spin-bearing centres is a less good strategy than using neutral radicals in designing coordination polymer magnets.

4. Experimental

4.1. General details

The general procedures adopted in the synthetic work were the same as those described in previous papers [9, 10]

4.2. Synthesis

4.2.1. 4'',4'''-Ditertbutyl-2',2'',2'''trimethoxy-{4-(4'-diphenylaminophenyl)pyridine} **(3)**

4-Bromopyridine hydrochloride (580 mg, 3.0 mmol) was added to a mixture of ethylene glycol 1,2-dimethyl ether (40 ml) and water (2 ml). Argon was bubbled through the mixture for 0.5 h. Tetrakis-triphenylphosphine palladium (0) (32 mg, 28 μmol) was added under a stream of argon. The boronic ester **2** (1.3 g, 2.5 mmol) [9] was dissolved in DME (10 ml) and degassed under a stream of argon for 0.5 h. The boronic ester solution was cannulated into the reaction vessel, barium hydroxide (1.54 g, 10 mmol) was finally added and the reaction mixture was refluxed for 48 h. The reaction was left to cool and the organic phase was extracted with dichloromethane (3 x 20 ml) washed with water (2 x 50 ml) and dried over anhydrous magnesium sulphate. Purification by flash chromatography gave *the amine* **3** as small light red crystals (1.1 g, 84 %). *Anal.* Calc. for $C_{34}H_{40}N_2O_3$: C, 77.82; H, 7.68; N, 5.33. Found: C, 77.50; H, 7.90; N, 5.20 %. MS (EI+) *m/z:* 524.1 (M^+, 100 %).m.p. 167.3°C. ^{1}H NMR (C_6D_6, 300 MHz) δ_H: 8.60 (2H, dd, *J* 7.2 and 1.55), 7.01 (2H, d, *J* 8.1), 7.0 (1H, m), 6.89 (2H, m), 6.86 (2H, d, *J* 2.14), 6.76 (2H, dd, *J* 8.2 and 2.2), 3.28 (12H, s, OMe), 3.17 (6H, s, OMe), 1.15 (36H, s, Bu). ^{13}C NMR (300 MHz, C_6D_6) δ_C: 154.2, 154.0, 153.8, 151.1, 147.9, 145.2, 140.5, 136.2, 126.1, 125.0, 121.3, 120.4, 118.6, 112.8, 111.8, 56.3, 56.2, 34.9, 32.0.

4.2.2. Manganese complex **(4)**

A solution of [Mn(hfac)$_2$.3H$_2$O] (45 mg, 0.068 mmol) was prepared in n-heptane (15 ml) by the addition of the minimum amount of dry diethyl ether (ca. 1 ml). To this solution was added a solution of ligand **3** (100 mg, 0.190 mmol) in dichloromethane (5 ml) under nitrogen. The resulting solution was left under a flow of nitrogen for 12 h. The resulting orange precipate was collected. The *complex* **4** was obtained as orange crystals (ca 90mg

crude) and recrystalised from THF/Hexane. *Anal*. Calc. for $C_{78}H_{82}N_4O_{10}F_{12}Mn$: C, 61.70; H, 5.44; N, 3.69. Found: C, 61.50; H, 5.35; N, 3.90 %.

4.2.3. Copper complex **(5)**

In the same manner the *complex* **5** was obtained as green crystals by recrystalisation from THF/Hexane. *Anal*. Calc. for $C_{78}H_{82}N_4O_{10}F_{12}Cu$: C, 61.35; H, 5.41; N, 3.67. Found: C, 61.20; H, 5.55; N, 3.40 %.

4.3. X-Ray crystallography

Crystallographic data for **3**, **4** and **5** were collected at 150K using a Nonius KappaCCDdiffractometer (with graphite-monochromated Mo-K_α radiation; λ = 0.71073 A˚) fitted with an Oxford Cryosystems nitrogen-cooled low-temperature device. Data processing for all structures was carried out using DENZO [29] while an absorption correction was applied using SORTAV [30]. The structures were all solved by direct methods and refined on F^2 using full matrix least-squares methods with SHELXL97 [31]. Hydrogen atoms were placed geometrically and treated with a riding model. Data is summarised in Table 1. In 4",4'"-di-tert-butyl-2',2",2'"trimethoxy-{4-(4'-diphenylaminophenyl)pyridine} **3,** the *tert*-butyl group centred on C27 is disordered and was modelled over two positions with relative occupancies of 0.71:0.29. The Mn atom in the complex **4** lies on a centre of inversion and so the asymmetric unit contains half the complex molecule together with two disordered molecules of THF. Each THF molecule was modeled over two positions with relative occupancies of 0.73:0.27 in one case and 0.72:0.28 for the other. The Cu atom in the complex **5** lies on a centre of inversion and so the asymmetric unit contains half the complex molecule together with two molecules of THF, one of

which is disordered. The disordered molecule was modeled over two positions with equal occupancies.

4.4 Cyclic voltammetry

These studies were carried out using a conventional three electrode system coupled to an EG&G Model 362 scanning potentiostat and the system was controlled by a PC unit running the 'Condecon 320' cyclic voltammetry software. The working electrode was a small platinum disc, ca. 2 mm diameter; the counter electrode was a platinum coiled wire and the reference electrode, a silver wire immersed in a saturated lithium chloride-dichloromethane mixture containing the supporting electrolyte tetrabutylammonium hexafluoroborate (0.1 M). Prior to use, solvents were thoroughly dried and degassed and the concentrations for the amines were approximately 1 mg cm^{-3}. The ferrocene/ ferrocenium couple (fast electron transfer) was used as a standard and its oxidation potential was checked before and after each experiment for the solvent used. For the voltammograms shown in Fig. 2 the potential was swept in the anodic direction (upper trace) and the lower trace represents the reverse sweep in the cathodic direction.

4.5. Ultra Violet/ visible/ near infra red spectroscopic studies

UV/Vis spectra in the range of 200-650 nm were recorded using a Perkin-Elmer Lambda 3000 UV/Vis/IR Spectrophotometer with a resolution of 0.1 nm in dichloromethane. Experiments were carried out using a pair of quartz cells with the corresponding solvent as reference. The path length of the cells was 10 mm. In a typical experiment, a dilute solution of the model diamine (1.6×10^{-5} mol. l^{-1}) in dichloromethane was titrated against a known concentration of $THBF_4$ (1 mol. l^{-1}), also in dichloromethane [15]. Ligand **3**, $\lambda_{max.}$ 354 nm, 3.50 eV ($\log_{10} \varepsilon$, 4.08); Radical cation $\mathbf{3}^{\cdot+}$, $\lambda_{max.}$ 467nm, 2.66 eV ($\log_{10} \varepsilon$, 4.01); 620, 2.02 (3.56); 920(s), 1.34 (3.75); Isosbestic points $\mathbf{3}/\mathbf{3}^{\cdot+}$, 297nm; 377. Complex **4**, $\lambda_{max.}$ 370 nm,

3.31 eV ($\log_{10}$ ε, 4.78); Diradical dication **4**$^{\cdot+}$, $\lambda_{max.}$ 354nm, 3.50 eV ($\log_{10}$ ε, 4.46); 469, 2.66 (4.58); 619, 2.00 (3.87); 925, 1.34 (4.01); Isosbestic point **4**/**4**$^{2,+}$, 419nm. Complex **5,** $\lambda_{max.}$ 369 nm, 3.40 eV ($\log_{10}$ ε, 4.56)

4.6. Magnetometry

Magnetic measurements were carried out using a SQUID magnetometer (MPMS, Quantum Design) at the University of Sheffield. Samples were prepared as a dilute frozen matrix using the same apparatus and combination of vacuum line and syringe techniques as previously described in detail in reference [9].

Appendix A. Supplementary data

CCDC 634674 contains the supplementary crystallographic data for the ligand **3,** CCDC 186580 contains the supplementary crystallographic data for the Mn complex **4,** .and CCDC 636674 contains the supplementary crystallographic data for the Cu complex **5.** .. These data can be obtained free of charge via http://www.ccdc.cam.ac.uk/conts/retrieving.html, or from the Cambridge Crystallographic Data Centre, 12 Union Road, Cambridge CB2 1EZ, UK; fax: (+44) 1223-336-033; or e-mail: deposit@ccdc.cam.ac.uk.

Acknowledgements

We thank EPSRC for funding this work and Dr H. Blythe (Physics, University of Sheffield) for assistance with the SQUID magnetometry.

References

[1] (a) A. Caneschi, D. Gatteschi, P. Rey and R. Sessoli, Inorg. Chem. 27 (1988) 1756;

(b) A. Caneschi, D. Gatteschi, J. P. Renard, P. Rey and R. Sessoli, Inorg. Chem. 28 (1989) 1976, 2940 and 3314.

[2] A. Caneschi, D. Gatteschi, R. Sessoli and P. Rey, Acc. Chem. Res. 22 (1982) 392.

[3] J. M. Manriquez, G. T. Yee, R. S. McLean, A. J. Epstein and J. S. Miller, Science 252 (1991) 1415.

[4] (a) K. Inoue and H. Iwamura, Chem. Commun. (1994) 2273 ;

(b) K. Inoue, T. Hayamizu, H. Iwamura, D. Hashizume and Y. Ohashi, J. Amer. Chem. Soc. 118 (1996) 1803.

[5] (a) K. Fegy, D. Luneau, E. Belorizky, M. Novac, J. L. Tholence, C. Paulsen, T. Ohm and P. Rey, Inorg. Chem. 37 (1998) 4524;

(b) K. Fegy, D. Luneau, C. Paulsen, T. Ohm and P. Rey, Angew. Cem. Internat. Edn. 37 (1998) 1270;

(c) A. Caneschi, D. Gatteschi, N. Lalioti, C. Sangregorio, R. Sessoli, G. Venturi, A. Vindigni, A. Rettori, M. G. Pini and M. A. Novak, Angew. Chem. Internat. Edn. 40 (2001) 1760;

(d) M. Minguet, D. Luneau, C. Paulson, E. Lhotel, A. Gorski, J. Waluk, D. B. Amabilino and J. Veciana, Polyhedron 22 (2003) 2349.

[6] (a) N. Koga, Y. Ishimaru and H. Iwamura, Angew. Chem. Internat. Edn. 35 (1996) 755;

(b) Y. Sano, M. Tanaka, N. Koga, K. Matsuda, H. Iwamura, P. Rabu and M. Drillon, J. Amer. Chem. Soc. **119** (1997) 8246 ;

(c) S. Karasawa, H Kumada, N. Koga and H. Iwamura, J. Amer. Chem. Soc. 123 (2001) 9685.

[7] Y. Takano, Y. Kitagawa, T. Onishi, Y. Yoshioka, K. Yamaguchi, N. Koga and H. Iwamura, J. Amer. Chem. Soc. 124 (2002) 450.

[8] W. T. Borden and E. R. Davidson, J. Amer. Chem. Soc. 99 (1977) 4587.

[9] R. J. Bushby, N. Taylor and R. A. Williams, J. Mater. Chem. 17 (2007) 955.

[10] R. J. Bushby, C. Kilner, N. Taylor and M. E. Vale, Tetrahedron, in press.

[11] (a) K. B. Oldham and J. Spanier, J Electroanal. Chem. 26 (1970) 331;
(b) K. B. Oldham, Anal. Chem. 44 (1972) 196;
(c) M. Grenness and K. B. Oldham, Anal. Chem. 44 (1972) 1121.

[12] Supplementary information.

[13] J. Britten, N. G. R. Hearns, K. E. Preuss, J. F. Richardson and S. Bin-Salamon, Inorg. Chem. 46 (2007) 3934.

[14] R. J. Bushby, D. R. McGill, K. M. Ng and N. Taylor, J. Chem. Soc., Perkin Trans. 2 (1997) 1405.

[15] B. Boduszek and H. J. Shine, J. Org. Chem. 53 (1988) 5142.

[16] S. Amthor, B. Noller and C. Lambert, Chem. Phys. 316 (2005) 141.

[17] B. Bleaney and K. D. Bowers, Proc. Roy. Soc. London Ser. A, 214 (1952) 451.

[18] H. Kumada, A. Sakane, N. Koga and H. Iwamura, J. Chem. Soc., Dalton Trans. (2000) 911.

[19] M. H. Dickman, L. C. Porter and R. J. Doedens, Inorg. Chem. 86 (1986) 2595.

[20] (a) K.Itoh in Magnetic Molecular Materials, ed. D. Gatteschi, O. Kahn, J. S. Miller, and F. Palacio, Kluwer, Dordrecht, 1991;

(b)M. M. Murray, P. Kaszynski, D. A. Kaisaki, W. H. Chang and D. A. Dougherty, J. Amer. Chem. Soc. 116 (1994) 8152;

(c) R. J. Bushby, D. R. McGill and K. M. Ng in Magnetism a Supermolecular Function, ed. O. Kahn, Kluwer, Dordrecht, 1996;

(d) P. M. Lathi in Magnetic Properties of Organic Materials, ed. P. M. Lathi, Marcel Dekker, New York, 1999;

(e) A. Rajca, J. Wongsriratanakul and S. Rajca, Science 294 (2001) 1503;

(f) N. A. Zaidi, S. R. Giblin, I. Terry and A. P. Monkman, Polymer 45 (2004) 5683.

[21] (a)A. H. Oka, T. Tamura, Y. Miura and Y. Teki, J. Mater. Chem. 11(2001) 1364;

(b) A. Rajca, Chem. Rev. 94 (1994) 871.

[22] D. A. Dougherty, Acc. Chem. Res. 24 (1991) 88.

[23] D. Maspoch, D. Ruiz-Molina, K. Wurst, J. Vidal-Gancedo and J. Veciana, Dalton Trans. (2004) 1073.

[24] (a) K. Itoh in Magnetic Molecular Materials, ed. D Gatteschi, O Kahn, J. S. Miller and F. Palacio, Kluwer, Dordrecht, 1991.

(b) K. Matsuda, N. Nakamura, K. Takahashi, K. Inoue, N. Koga and H. Iwamura, Molecule-Based Magnetic Materials, ACS Symposium Series 644 (1996) 142.

[25] J. Veciana, C. Rovira, M. I. Crespo, O. Armet, V. M. Domingo, and F. Palacio, J. Amer. Chem. Soc. 113 (1991) 2552.

[26] S. Karasawa, H. Kumada, N. Koga and H. Iwamura, J. Amer. Chem. Soc., 123 (2001) 9685.

[27] This work.

[28] (a) R. J. Bushby, D. Gooding, M. Thornton-Pett, and M. E. Vale, Mol. Cryst. Liquid Cryst. 334 (1999) 167;

(b) R. J. Bushby, D. Gooding, and M. E. Vale, Phil. Trans. Roy. Soc. A 357 (1999) 2939;

(c) R. J. Bushby in Magnetism: Molecules to Materials II, Molecule-Based Materials, ed. J. S. Miller and M. Drillon, Wiley, New York, 2001.

[29] Z. Otwinowski and W. Minor, Methods Enzymol. 276 (1997) 307.

[30] R. H. Blessing, Acta Crystallogr., Sect. A 51 (1995) 33.

[31] G.M.Sheldrick, SHELXL-97 Program for the Refinement of Crystal Structures, University of Gottingen, Germany, 1997.

Table 1**.** Crystallographic data for compounds **3-5**.

Scheme 1. Synthesis of the complexes: Reagents (i) n-BuLi/ THF/ -78°C; (ii) $B(O^iPr)_3$/ THF/ -78°C; (iii) H^+/ H_20/ -78°C; (iv) Pinacol/ 4Å molecular sieve/ Δ, 46% (overall); (v) 4-bromopyridine hydrochloride/ $Pd(PPh_3)_4$/ $Ba(OH)_2$/ DME/ Ar atmos./ Δ; (vi) $[Cu(hfac)_2]$ or $[Mn(hfac)_2]$/ heptane/ ether/ DCM.

Fig. 1. X-ray derived structures of the ligand **3** (top), manganese complex **4** (middle) and copper complex **5** (bottom). For the complexes the Mn and Cu are on inversion centres. Ellipsoid probabilities are 50%.

Fig. 2. (left) Cyclic voltammogram for 10^{-3} M solutions of ligand **3** in DCM with 0.1 M tetrabutylammonium hexafluorophosphate as the supporting electrolyte. Potential relative to Ag/AgCl. (right) Corresponding deconvoluted d*I*//dE plot. Sweep rate 500 mVs^{-1} .

Fig. 3. (top) Ultra Violet/ visible/ near infra red spectra for the oxidation for monopyridyl ligand **3** to the radical cation species $\mathbf{3}^+$. (bottom) UV spectra for the oxidation for Mn complex **4** to the diradical dication species $\mathbf{4}^{2+}$. Oxidation performed in dichloromethane using $THBF_4$ at room temperature.

Fig. 4. (top) 'Curie' law plot of the reciprocal of magnetic susceptibility (χ) vs. temperature for a frozen dilute solution of the radical cation $\mathbf{4}^{\cdot+}$. (middle) Plot of product of susceptibility and temperature (χT vs T) fitted to the Bleaney Bowers equation. (bottom) Plot of normalized magnetisation vs. ratio of field and temperature (Brillouin plot).

Fig. 5. (top) 'Curie' law plot of the reciprocal of magnetic susceptibility (χ) vs. temperature for a frozen dilute solution of the diradical dication $\mathbf{4}^{2.+}$. (middle) Plot of product of susceptibility and temperature (χT vs T) fitted to the Bleaney Bowers equation. (bottom) Plot of normalized magnetisation vs. ratio of field and temperature (Brillouin plot).

Fig. 6. Schematic of the parallels between spin-coupling pathways in high-spin organic polymers and those in coordination polymer molecular magnets (see text).

Table 1. Crystallographic data for compounds **3-5**.

Data	**3**	**4**	**5**
Formula	$C_{34}H_{40}N_2O_3$	$C_{94}H_{114}F_{12}MnN_4O_{14}$	$C_{94}H_{114}CuF_{12}N_4O_{14}$
Formula weight	524.68	1806.83	1815.43
Crystal system	Monoclinic	Triclinic	Triclinic
Space group	*C*2/*c*	$P\bar{1}$	$P\bar{1}$
a (Å)	17.2432(3)	11.9670(2)	11.8763(2)
b (Å)	17.0393(3)	13.9279(3)	13.9797(3)
c (Å)	20.5000(4)	15.5052(4)	15.4469(3)
α (º)	90	83.1310(10)	81.8890(10)
β (º)	97.005(2)	74.3390(10)	73.0810(10)
γ (º)	90	66.5150(10)	66.5500(9)
V (Å^3)	5978.2(2)	2282.05(9)	2250.02(8)
Z	8	1	1
ρ_{calc} (g cm^{-3})	1.166	1.315	1.340
μ (mm^{-1})	0.074	0.233	0.333
T (K)	150(2)	150(2)	150(2)
Measured reflections	46881	43394	43337
Independent reflections	5838	8913	8847
*R*int	0.0963	0.0643	0.0719
R(*F*) [a] [$I > 2\sigma(I)$]	0.0642	0.0536	0.0591
wR(F^2) [b] (all data)	0.1787	0.1440	0.1672
$\Delta\rho_{min,max}$ (e Å^{-3})	-0.230, 0.406	-0.490, 0.566	-0.628, 1.082

[a] $R = \Sigma [|F_o| - |F_c|] / \Sigma |F_o|$. [b] $wR = [\Sigma w(F_o^2 - F_c^2)/ \Sigma wF_o^4]^{1/2}$

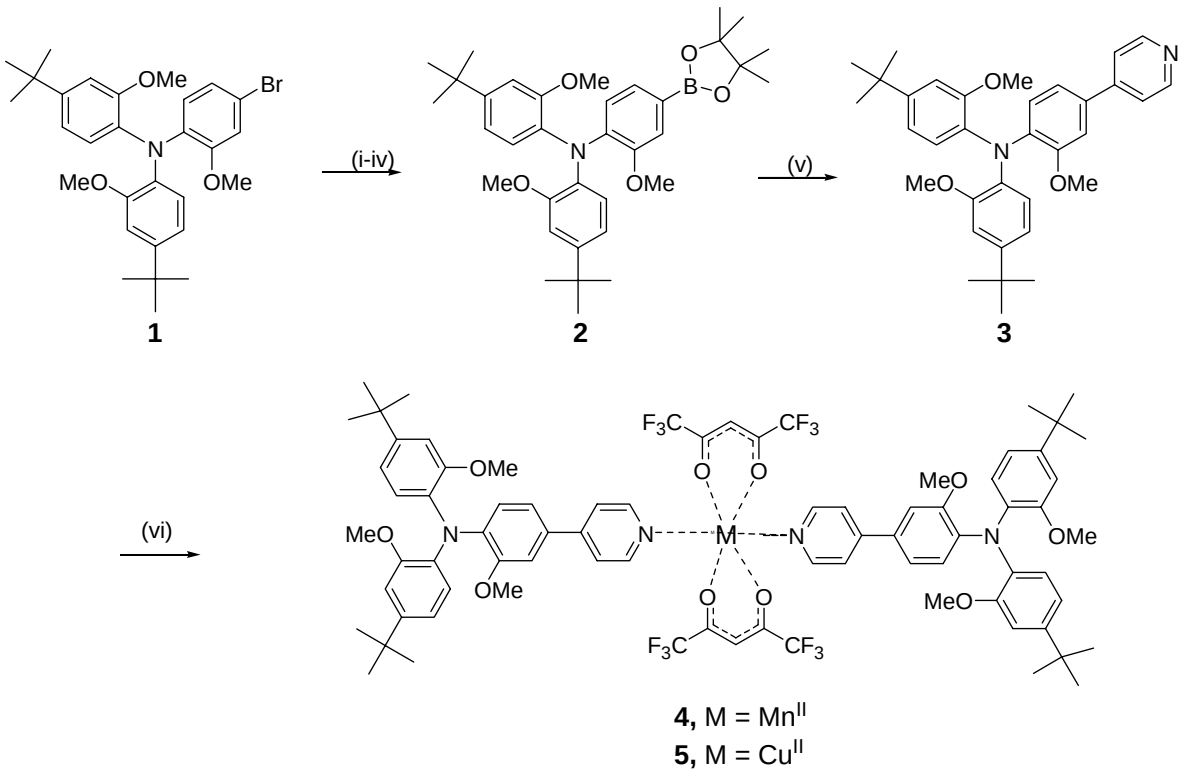

Scheme 1. Synthesis of the complexes: Reagents (i) n-BuLi/ THF/ -78°C; (ii) $B(O^iPr)_3$/ THF/ -78°C; (iii) H^+/ H_20/ -78°C; (iv) Pinacol/ 4Å molecular sieve/ Δ, 46% (overall); (v) 4-bromopyridine hydrochloride/ $Pd(PPh_3)_4$/ $Ba(OH)_2$/ DME/ Ar atmos./ Δ; (vi) $[Cu(hfac)_2]$ or $[Mn(hfac)_2]$/ heptane/ ether/ DCM.

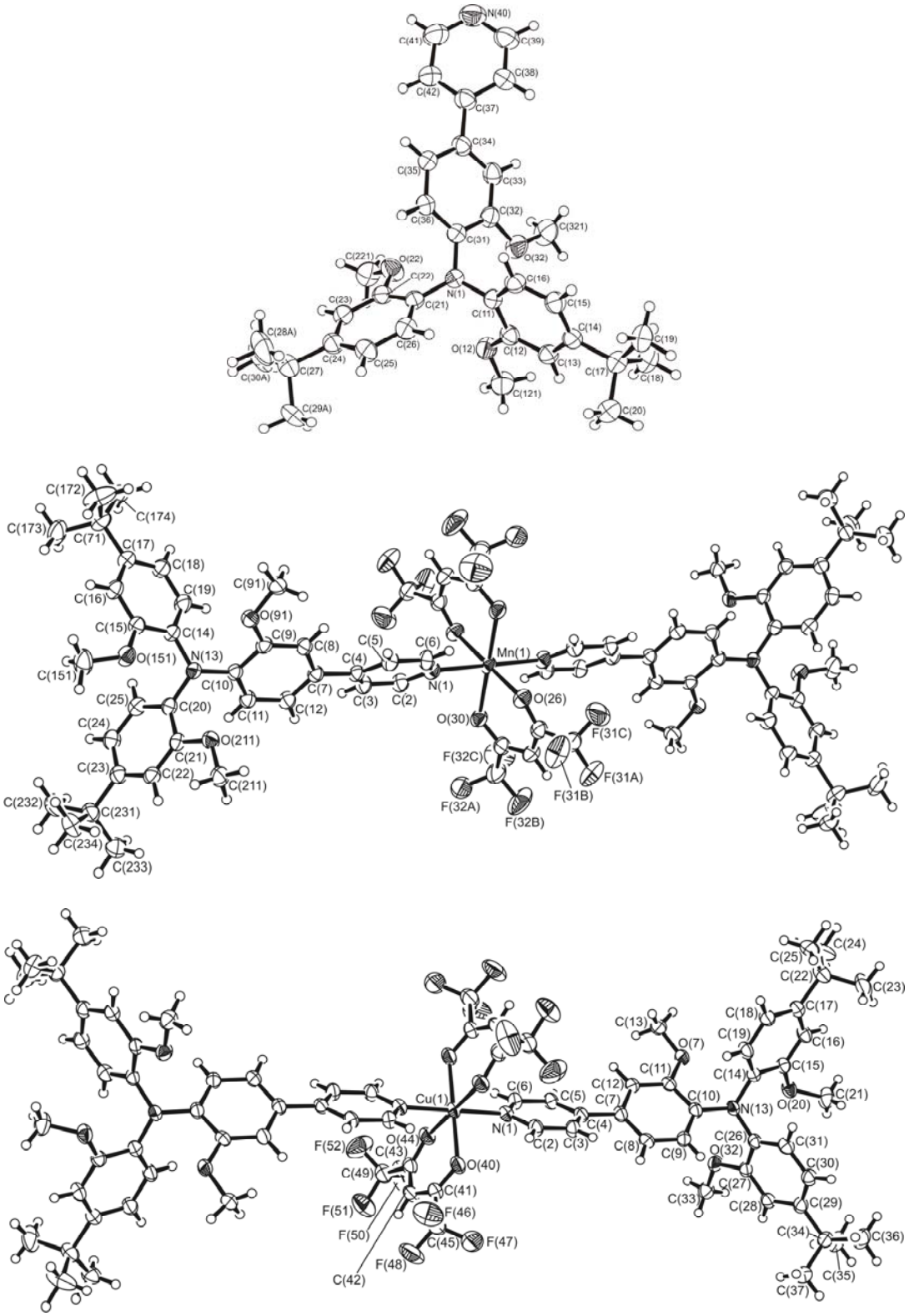

Fig. 1. X-ray derived structures of the ligand **3** (top), manganese complex **4** (middle) and copper complex **5** (bottom). For the complexes the Mn and Cu are on inversion centres. Ellipsoid probabilities are 50%.

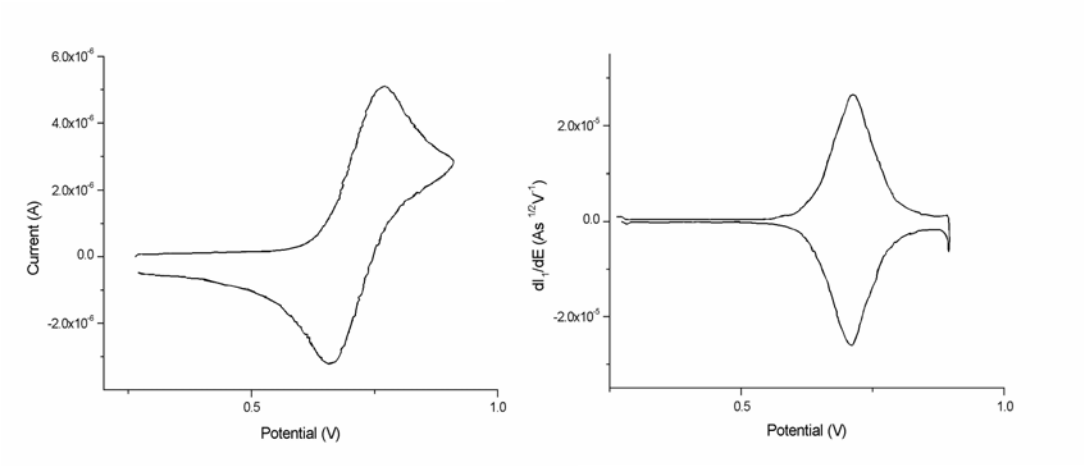

Fig. 2. (left) Cyclic voltammogram for 10^{-3} M solutions of ligand **3** in DCM with 0.1 M tetrabutylammonium hexafluorophosphate as the supporting electrolyte. Potential relative to Ag/AgCl. (right) Corresponding deconvoluted d*I*//dE plot. Sweep rate 500 mVs^{-1}

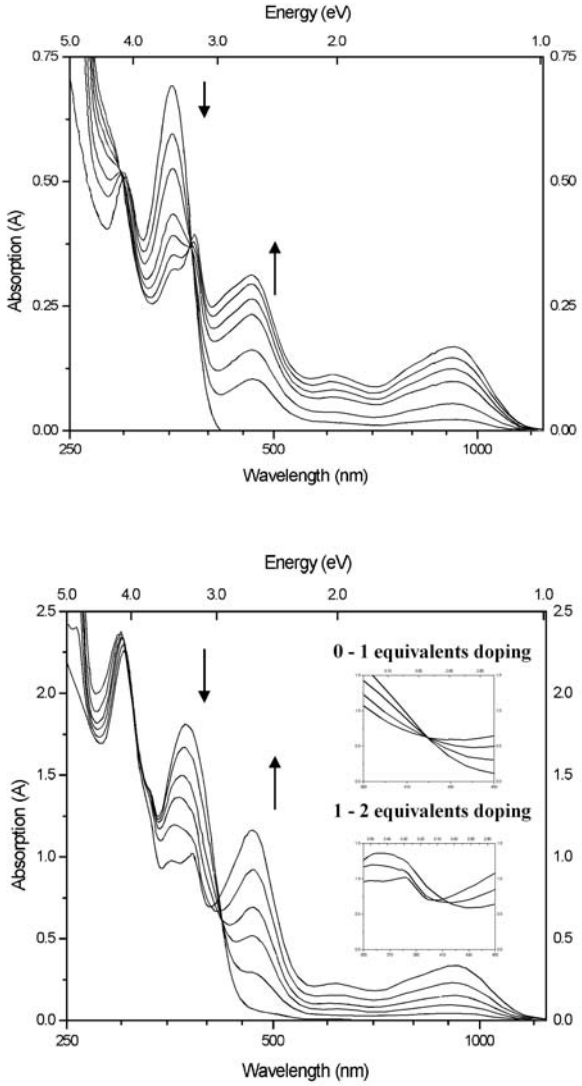

Fig. 3. (top) Ultra Violet/ visible/ near infra red spectra for the oxidation for monopyridyl ligand **3** to the radical cation species $\mathbf{3}^{+}$. (bottom) UV spectra for the oxidation for Mn complex **4** to the diradical dication species $\mathbf{4}^{2+}$. Oxidation performed in dichloromethane using $THBF_4$ at room temperature.

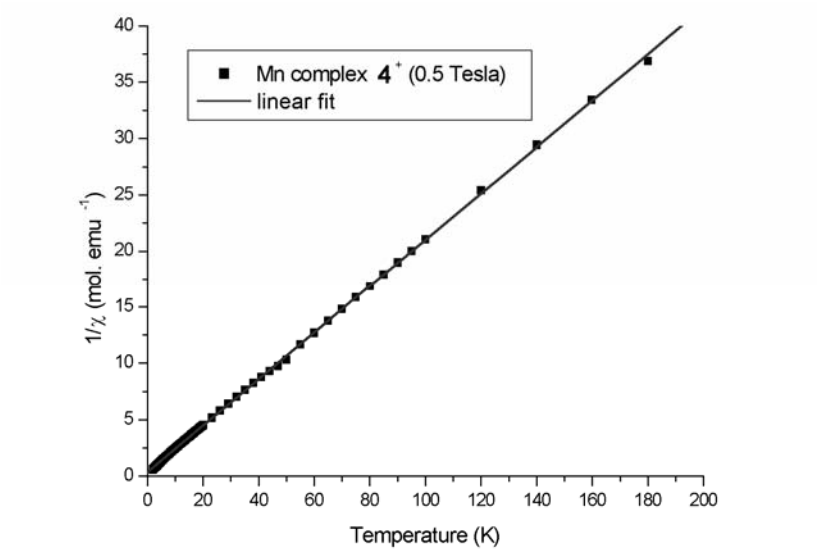
Mn complex 4+ (0.5 Tesla)
linear fit
1/χ (mol. emu-1)
Temperature (K)

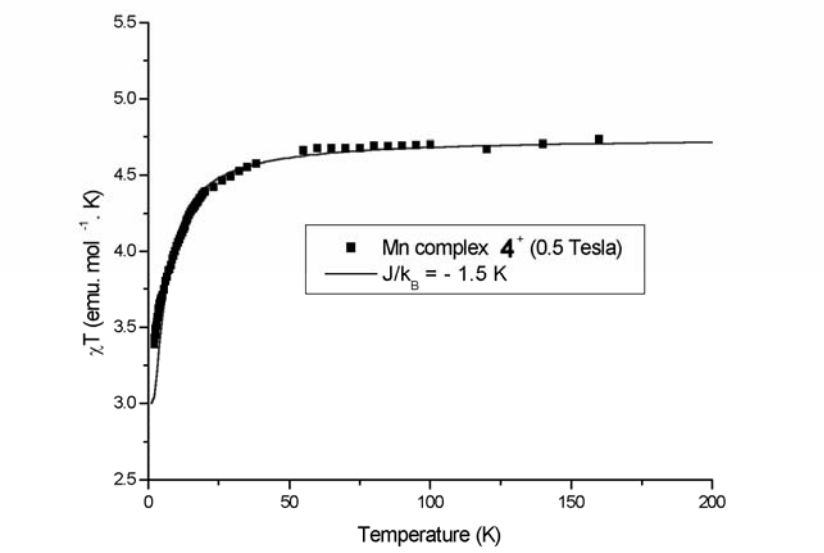
Mn complex 4+ (0.5 Tesla)
J/kB = - 1.5 K
χT (emu. mol-1. K)
Temperature (K)

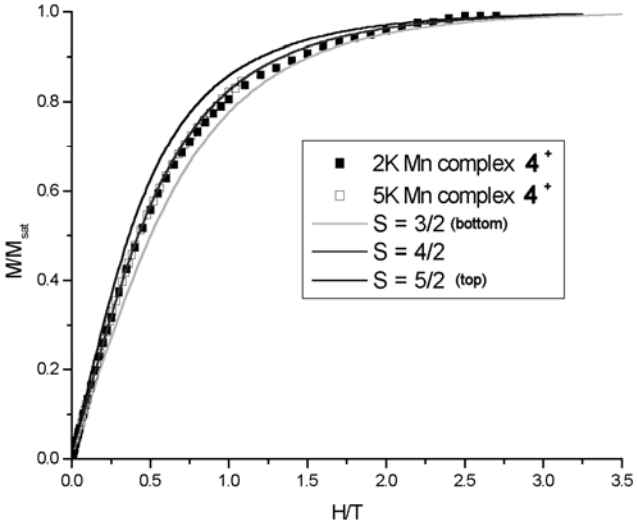
2K Mn complex 4+
5K Mn complex 4+
S = 3/2 (bottom)
S = 4/2
S = 5/2 (top)
M/Msat
H/T

Fig. 4. (top) 'Curie' law plot of the reciprocal of magnetic susceptibility (χ) vs. temperature for a frozen dilute solution of the radical cation $\mathbf{4}^{\bullet+}$. (middle) Plot of product of susceptibility and temperature (χT vs T) fitted to the Bleaney Bowers equation. (bottom) Plot of normalized magnetisation vs. ratio of field and temperature (Brillouin plot).

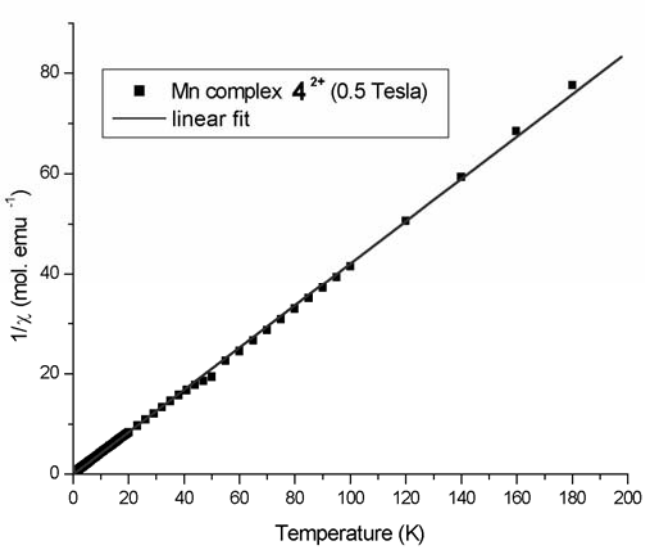
Mn complex 4 2+ (0.5 Tesla)
linear fit
1/χ (mol. emu -1)
Temperature (K)

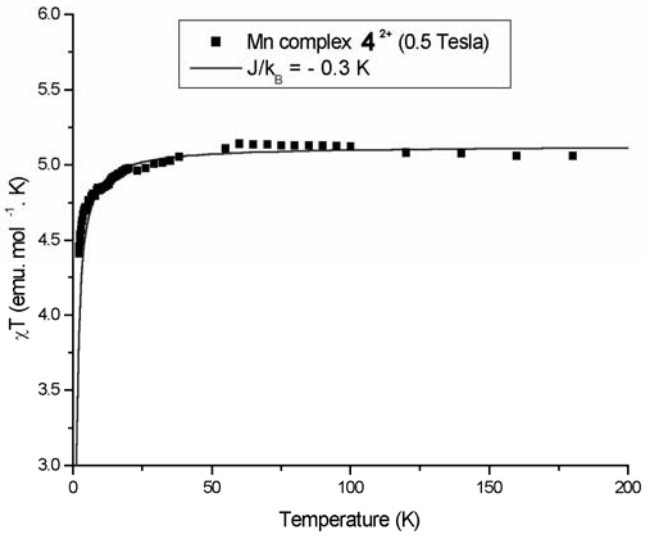
Mn complex 4 2+ (0.5 Tesla)
J/kB = - 0.3 K
χT (emu. mol -1. K)
Temperature (K)

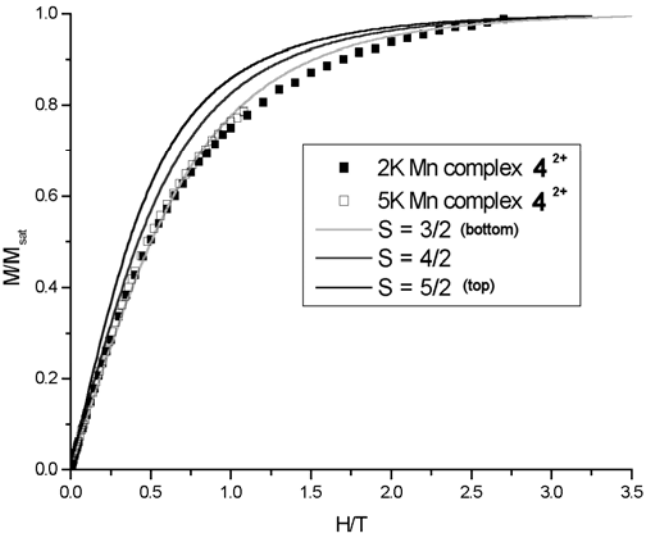
2K Mn complex 4 2+
5K Mn complex 4 2+
S = 3/2 (bottom)
S = 4/2
S = 5/2 (top)
M/Msat
H/T

Fig. 5. (top) 'Curie' law plot of the reciprocal of magnetic susceptibility (χ) vs. temperature for a frozen dilute solution of the diradical dication $\mathbf{4}^{2\bullet+}$. (middle) Plot of product of susceptibility and temperature (χT vs T) fitted to the Bleaney Bowers equation. (bottom) Plot of normalized magnetisation vs. ratio of field and temperature (Brillouin plot).

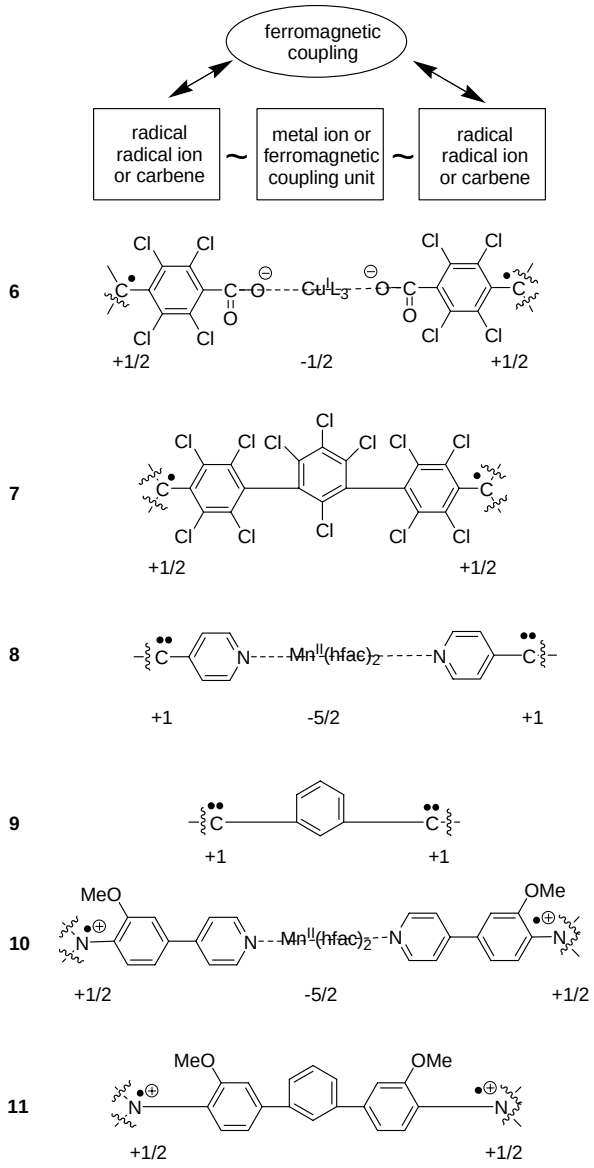

Fig. 6. Schematic of the parallels between spin-coupling pathways in high-spin organic polymers and those in coordination polymer magnets (see text).